$BaCe_{1-x-y}Zr_xY_yO_{3-\delta}$ Proton Conductors: the Role of the Synthetic Route on Their Properties

S. Barison[a], M. Battagliarin[a], S. Boldrini[b], G. Chiodelli[c], L. Doubova[a], M. Fabrizio[a], R. Gerbasi[d], L. Malavasi[c], C. Mortalò[a]

[a] IENI-CNR, Corso Stati Uniti 4 - 35127 Padova- Italy
[b] ISIB-CNR, Corso Stati Uniti 4-35127 Padova - Italy
[c] IENI-CNR, Viale Taramelli 16 - 27100 Pavia- Italy
[d] ICIS-CNR, Corso Stati Uniti 4 - 35127 Padova- Italy

Proton conducting electrolyte materials are promising candidates for the development of low temperature solid oxide fuel cells. Among them, various doped barium cerate compounds, such as $BaCe_{1-x}Y_xO_{3-\delta}$, have been intensively investigated because of their high proton conductivity. As a drawback, cerates are chemically unstable in CO_2-containing atmospheres, such as in case of hydrocarbon or syngas fuelled fuel cells. Conversely, doped barium zirconates electrolyte materials exhibit high chemical stability but lower proton conductivity. A goal of this work was to obtain full-density proton conducting materials having both high conductivity and good chemical stability. In particular, the compositions investigated in this work were $BaCe_{1-x-y}Zr_xY_yO_{3-\delta}$ (x=0, 0.1, 0.2, 0.3, 0.4; y=0.15, 0.20). The partial substitution of Ce by Zr in doped barium cerate considerably increased their chemical stability in CO_2 atmosphere without sensibly affecting the conductivity.

Introduction

Solid oxide fuel cells (SOFCs) have gained much attention as promising energy conversion systems, due to their high thermodynamic efficiency and low impact to the environment (1). Nevertheless, the most important issue for their commercialization is lowering their conventional operating temperatures to the 400-700°C range. In view of this, proton conducting electrolyte materials having perovskite structure are promising candidates for the development of low temperature SOFCs. Among them, various doped barium cerate compounds, such as $BaCe_{1-x}Y_xO_{3-\delta}$, have been intensively investigated and showed high proton conductivity (2). As a drawback, cerates are chemically unstable in CO_2-containing atmospheres, such as in case of hydrocarbon or syngas fuelled SOFCs (3). On the contrary, doped barium zirconates exhibit higher chemical stability but lower proton conductivity.

On the basis of these remarks, recent studies have shown that the partial substitution of Ce by Zr in Y doped barium cerates ($BaCe_{1-x-y}Zr_xY_yO_{3-\delta}$) considerably improved the chemical stability of these materials in CO_2 atmosphere (4). The stabilization effect increased with Zr content and was ascribed to the Gibbs free energy change for the reactions of the solid solution of $BaCeO_3$ and $BaZrO_3$ with CO_2 (4). Solid solutions with substitution of 20 or 30% of cerium showed both suitable proton conductivity and good chemical stability (5). Nevertheless, a hindrance to the application of these solid solutions as electrolytes in electrode-supported devices is the need for high sintering temperatures

for their densification (1500-1800°C), which could cause the detrimental sintering of the supporting electrodes. Moreover, the exposure of these materials to elevated temperatures induced a barium deficiency due to the BaO vaporization, leading to significantly lower conductivities than stoichiometric compositions (5). In this work, a modified sol-gel Pechini process has been exploited, where the use of EDTA and ethylene glycol as chelating and polymerizing agents respectively has been inspected in order to ensure homogeneous mixing of metallic cations at a molecular level and improve the powder morphology in order to reduce the sintering temperatures.

Therefore, the goal of this work has been the synthesis by a modified sol-gel Pechini method of solid solutions having composition $BaCe_{1-x-y}Zr_xY_yO_{3-\delta}$ (x=0, 0.1, 0.2, 0.3, 0.4; y=0.15, 0.20). On the considered solid solutions, an extensive structural and morphological investigation by means of X-Ray Diffraction (XRD) and Scanning Electron Microscopy (SEM) has been performed. The study of the conductivity performance in protonic and ionic conditions was performed by means of Electrochemical Impedance Spectroscopy (EIS) technique.

Experimental

Powders of cerate-zirconate solid solutions having nominal composition $BaCe_{1-x-y}Zr_xY_yO_{3-\delta}$ (x=0, 0.1, 0.2, 0.3, 0.4; y=0.15, 0.20, hereafter BCY15, BCZ10Y15, BCZ20Y20, etc.) have been prepared by a sol-gel modified Pechini process. The starting materials were $Ba(NO_3)_2$ (Sigma-Aldrich, 99+%), $Ce(NH_4)_2(NO_3)_6$ (Alfa Aesar, 99.5%), $ZrO(NO_3)_2{\cdot}2.35\ H_2O$ (Alfa Aesar, 99.9%), $Y(NO_3)_3{\cdot}6H_2O$ (Alfa Aesar, 99.9%) as metal precursor and EDTA (ethylenediaminetetraacetic acid, Sigma-Aldrich, 99+%) and ethylene glycol (Aldrich, 99+%) as complexing and polymerizing agents respectively. The water content of zirconium salt was determined by thermogravimetric analysis. Ammonium hydroxide (Riedler de Haën, NH_3 33%) was added to promote the dissolution of EDTA in deionized water (Millipore, Billerica MA, USA). A barium excess (10 mol%) was introduced in the synthesis to overcome an eventual barium deficiency. The temperatures for the thermal treatments of the gel were chosen on the base of thermogravimetric analyses: simultaneous differential thermal analysis and thermogravimetry (DTA/TGA) were carried out on reagents, gel precursors and on the final products using a TA Instruments SDT Q600 Analyzer.

The final BCZY powders were obtained by calcination in air at temperatures ranging between 1100 and 1250 °C, depending on Zr content. The resulting powders were axially pressed in form of pellets and sintered for 10 hours in air at temperatures ranging between 1300 and 1450°C. Samples density was estimated by measuring the pellets weight and dimensions and this value was compared with the theoretical density based on crystal lattice parameters.

X-ray powder diffraction (XRPD) patterns were recorded at room temperature using a Philips PW 1830 diffractometer with Bragg-Brentano geometry, employing a Cu anode X-ray tube operated at 40 kV and 30 mA. NiO powder was used as internal standard. Morphological investigations were carried out by SEM observations with a JSM5600LV model (Jeol Ltd, Japan). AC electrical characterizations were made by using the Autolab potentiostat/galvanostat model PGSTAT100. Conductivity measurements were performed in both dry O_2 and 5%H_2/Ar humidified atmospheres.

Results and discussion

The modified Pechini sol-gel process described in this work ensured homogeneous mixing of metal cations at a molecular level. In fact, the strong chelating power of EDTA promoted the uniformity of metal ion distribution (6), affected the powder morphology and reduced the amount of organic precursor respect to citric acid, commonly employed in Pechini method (7). Single phase perovskite powders were obtained in the whole composition range (see Figure 1) and a linear reduction of the unit cell dimension with increasing the Zr atomic percentage was detected.

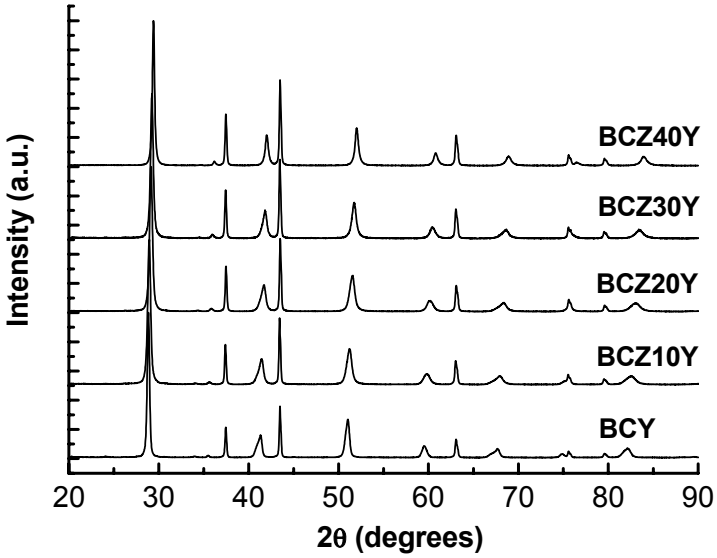

Figure 1. XRD patterns for the BCZY15 powders having different Zr amount (Zr=0, 0.10, 0.20, 0.30, 0.40). NiO was introduced as a reference.

SEM observations (see Figure 2a,b) confirmed that the modified Pechini process favoured the formation of sub-micrometric powders (particles sizes between 100-200 nm aggregated in open, sponge-like structures) (8). Thanks to small grain sizes, full-density pellets (densities ≥ 92% of theoretical ones) were achieved at sintering temperatures ranging between 1250 and 1450°C depending on Zr content, thus lowering the temperatures with respect to ones commonly used in other preparation routes (≥ 1600°C). SEM micrographs showed grain coarsening with homogeneous distribution of the grain sizes (see Figure 2c,d).

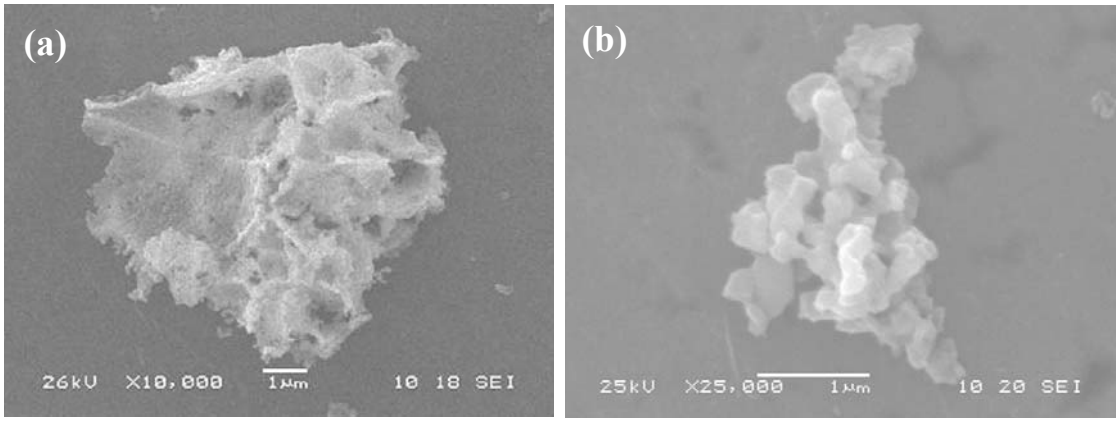

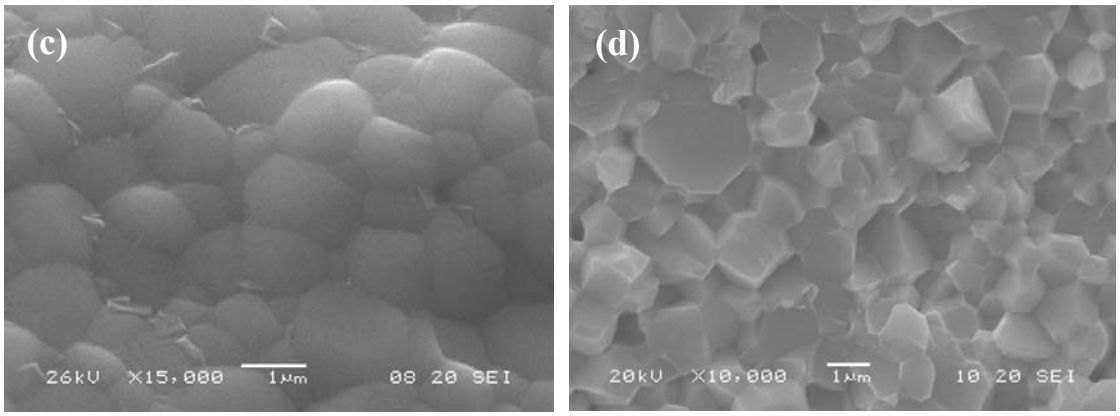

Figure 2. SEM micrographs of a) BCY20 powder treated at 1100°C; b) BCZ40Y15 powder treated at 1250°C; c) BCY20 sintered at 1250°C ($D_{exp}/D_{theor} \approx 92.5\%$); d) BCZ40Y15 sintered at 1450°C ($D_{exp}/D_{theor} \approx 94.4\%$).

The study by means of EIS technique of the conductivity performance in protonic and ionic conditions at low temperatures (100-350°C) was used to probe the relative contribution of bulk and specific grain conductivity (5) to the total conductivity of the samples. In fact, although at typical fuel cell operating temperatures the grain boundary contribution to the impedance response is minor, in order to optimize the synthesis and sintering processes and to study the materials properties it is extremely advantageous to correlate, both qualitatively and quantitatively, the conductivity at low temperatures to the microstructural features (determined by SEM) that characterize the sintered samples. Moreover, the grain boundaries may play an important role in the molecular diffusion of water (5). Figure 3 reports the bulk and specific grain boundary conductivities in the 100-350°C temperature range for BCY20 in dry O_2 atmosphere. The activation energy for transport through grain boundaries is higher than that for transport through bulk.

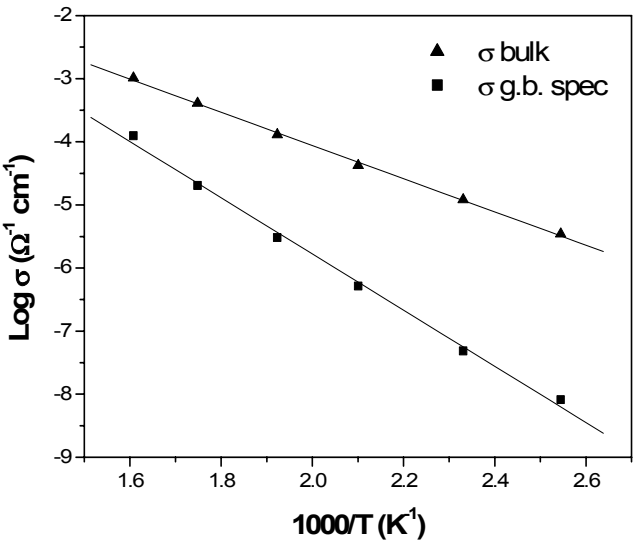

Figure 3. Bulk and specific grain boundary conductivities of BCY20 in dry O_2 atmosphere for the 100-350°C temperature range.

Our previous investigation on the conductivity in the 100-900°C temperature range of $BaCe_{1-y}Y_yO_{3-\delta}$ (y=0, 0.1, 0.15 and 0.2) pellets prepared by a sol-gel process has shown

significantly high proton conductivities (9). The highest values (> 10^{-2} $\Omega^{-1}cm^{-1}$ in H_2/H_2O atmosphere at 550°C) were found for x=0.15 and x=0.20 compositions. Figure 4 shows the conductivity depending on 1000/T for BCY15 and BCY20 in both environments (dry O_2 and humidified 5%H_2/Ar).

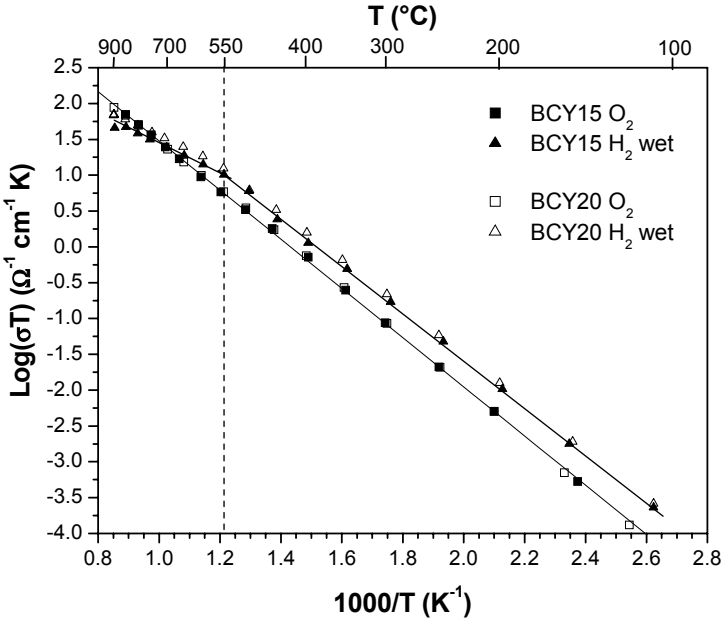

Figure 4. Arrhenius plots of conductivity for BCY15 and BCY20 in dry O_2 and humidified 5%H_2/Ar atmosphere.

An interesting feature of these Arrhenius plots is a clear slope change around 550°C in the humidified H_2 environment, while no changes were observed in O_2 atmosphere. This slope change could be probably related to a BCY phase transition in H_2 humidified environment observed also by neutron power diffraction for $BaCe_{1-x}Y_xO_{3-\delta}$ ($0 \leq x \leq 0.3$) (10), which may induce a change in the conductivity mechanism, and/or to a loss of charge carriers (water) at temperatures between 500 and 600°C.(11) An extensive investigation on the correlation between BCY structure and proton transport properties at different temperatures is ongoing.

Regarding sintered $BaCe_{1-x-y}Zr_xY_yO_{3-\delta}$ samples, the Y content was kept at y=0.15 and 0.20. Figure 5 reports the conductivities in H_2/H_2O environment, registered for BCZY15 having different Zr amount (the measurements in O_2 environment are ongoing). As observable in Figure, the partial Ce substitution with Zr induced a slight decrease on the conductivities at high temperatures, while almost no influence was observed at intermediate temperatures and slight effect at low temperatures. Therefore, although BYZ is highly refractory with low rates of grain growth under typical sintering conditions (12) and, therefore, the Ce substitution with Zr could led to a lowering of densities and conductivities, the sol-gel process permitted to achieve materials having high densities at sintering temperatures lower than ones typically used for these materials (≥1600°C), leading to higher conductivities.

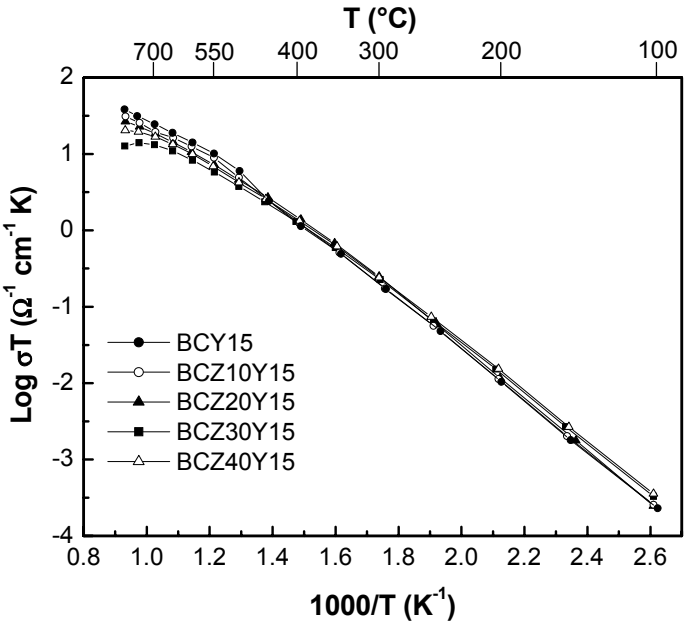

Figure 5. Arrhenius plots of conductivity for BCZY15 having different Zr amount, measured in humidified 5%H_2/Ar atmosphere.

As observable in Figure, the conductivity was weakly reduced with increasing of Zr content. As an example, at 500°C the conductivity changed from 0.0078 Ω^{-1} cm^{-1} for BCY15 to 0.0055 Ω^{-1} cm^{-1} for BCZ40Y15. The activation energies (E_a) varied with temperatures: at low temperatures (< 350°C) the E_a is around 0.65 eV and slightly decreased with increasing Zr content, while at higher temperatures (350-600 °C) the E_a drop off to values around 0.4-0.6 eV, depending on Zr content. An extensive study on the activation energies and the related phenomena is ongoing.

As predicted by the high stability of zirconates in CO_2-containing atmosphere, the BCZY powders showed an increase on phase stability with increasing of Zr content. In fact, thermogravimetric analyses performed in N_2/CO_2 flux showed a remarkable weight uptake for BCY (≈12 wt%) and BCZ10Y samples (≈11 wt%), while a sharp decrease on weight gain was observed when 20% of Ce was substituted with Zr (weight uptake < 1% for BCZ20Y). In the case of BCZ30Y and BCZY40Y samples the weight change was negligible, confirming the high stability of these materials. As observed in Figure 6, TGA curves showed a weight gain around 500-600°C, indicating that reaction with CO_2 has occurred. Further heating induced weight loss around 1000-1200°C, implying that reverse reaction has taken place and CO_2 has been lost. During subsequent cooling phase, these materials remained stable up to around 800-900°C, at which point they again reacted with CO_2, as evidenced by an increase in weight.

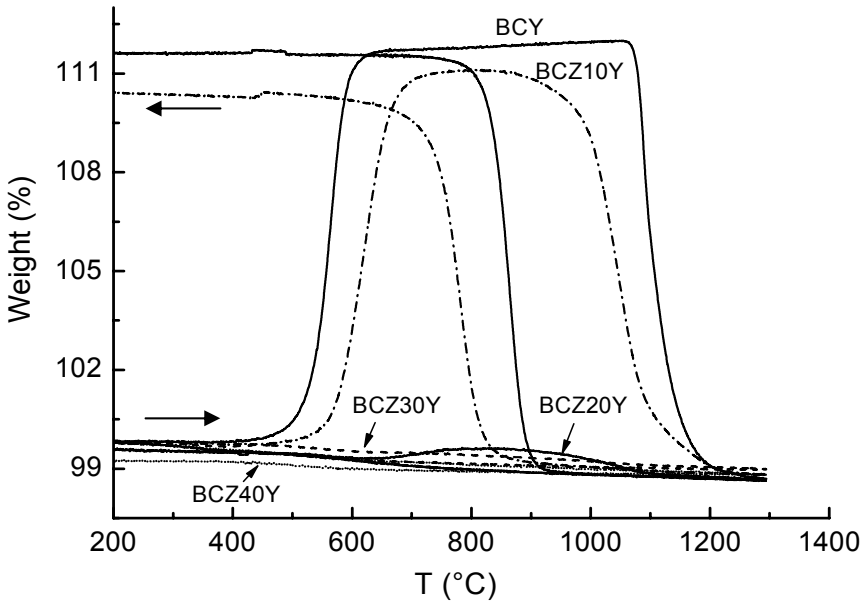

Figure 6. TGA curves for BCZY15 samples in N_2/CO_2 atmosphere (N_2=100 ml/min, CO_2=20 ml/min).

To conclude, thanks to the high densities obtained in this work the $BaCe_{1-x-y}Zr_xY_yO_{3-\delta}$ materials showed high proton conductivities, only slightly influenced by the Zr amount. Moreover, a significant improvement on the chemical stability was observed for BCZY materials having Zr≥0.20. Therefore, these perovskite materials seem promising candidates as electrolytes in hydrocarbon fueled proton conducting SOFCs. The development of this work will be the optimization of screen printing procedure to deposit electrolyte films based on these materials on supporting anodes, in order to study their performances.

Acknowledgments

This research has been funded by the *"Celle a combustibile ad elettroliti polimerici e ceramici: dimostrazione di sistemi e sviluppo di nuovi materiali"* FISR Project of Italian MUR.

References

1. B.C.H. Steele, A. Heinzel, *Nature*, **414**, 345 (2001).
2. H. Iwahara, *Solid State Ionics*, **77**, 289 (1995).
3. N. Bonanos, K.S. Knight, B. Ellis, *Solid State Ionics*, **79**, 161 (1995).
4. K.H. Ryu, S. M. Haile, *Solid State Ionics*, **125**, 355 (1999).
5. S.M. Haile, G. Staneff, K.H. Ryu, *J. Mater. Sci.*, **36**, 1149 (2001).
6. V. Agarwal, M. Liu, *J. Mater. Sci.*, **32**, 619 (1997).
7. M.P. Pechini, *U.S. Patent* 3,330,697*,* 1967.
8. S. Barison, M. Battagliarin, S. Daolio, M. Fabrizio, E. Miorin, P.L. Antonucci, S. Candamano, V. Modafferi, E.M. Bauer, C. Bellitto, G. Righini, *Solid State Ionics,* **177,** 3473 (2007).
9. G. Chiodelli, L. Malavasi, C. Tealdi, S. Barison, M. Battagliarin, L. Doubova, M. Fabrizio, C. Mortalò, R. Gerbasi, submitted to *J. Mater. Sci.*.

10. K. Takeuchi, C.K. Loong, J.W. Richardson Jr., J. Guan, S.E. Dorris, U. Balachandran, *Solid State Ionics,* **138**, 63 (2000).
11. A. Kruth, J.T.S. Irvine, *Solid State Ionics,* **162–163,** 83 (2003).
12. P. Babilo and S.M. Haile *J. Am. Ceram. Soc.* **88,** 2362 (2005).